Journal of Hydrology 558 (2018) 115–128

Contents lists available at ScienceDirect

Journal of Hydrology

journal homepage: www.elsevier.com/locate/jhydrol

Research papers

Fill and spill drives runoff connectivity over frozen ground

A.E. Coles [*,1], J.J. McDonnell

Global Institute for Water Security, School of Environment and Sustainability, University of Saskatchewan, 11 Innovation Boulevard, Saskatoon, SK S7N 3H5, Canada

ARTICLE INFO

Article history:
Received 18 May 2017
Received in revised form 4 January 2018
Accepted 7 January 2018
Available online 11 January 2018
This manuscript was handled by Tim R. McVicar, Editor-in-Chief, with the assistance of Dawen Yang, Associate Editor

Keywords:
Hydrological connectivity
Snowmelt
Frozen ground
Runoff generation
Fill and spill

ABSTRACT

Snowmelt-runoff processes on frozen ground are poorly understood at the hillslope scale. This is especially true for hillslopes on the northern Great Plains of North America where long periods of snow-covered frozen ground with very shallow slopes mask any spatial patterns and process controls on connectivity and hillslope runoff generation. This study examines a 4.66 ha (46,600 m^2) hillslope on the northern Great Plains during the 2014 spring snowmelt season to explore hillslope runoff processes. Specifically, we explore the spatial patterns of runoff production source areas and examine how surface topography and patterns of snow cover, snow water equivalent, soil water content, and thawed layer depth – which we measured on a 10 m grid across our 46,600 m^2 hillslope – affect melt water partitioning and runoff connectivity. A key question was whether or not the controls on connectivity are consistent with the fill and spill mechanism found in rain-dominated and unfrozen soil domains. The contrast between the slow infiltration rates into frozen soil and the relatively fast rates of snowmelt delivery to the soil surface resulted in water accumulation in small depressions under the snowpack. Consequently, infiltration was minimal over the 12 day melt period. Instead, nested filling of micro- and meso-depressions was followed by macro-scale, whole-slope spilling. This spilling occurred when large patches of ponded water exceeded the storage capacity behind downslope micro barriers in the surface topography, and flows from them coalesced to drive a rapid increase in runoff at the hillslope outlet. These observations of ponded water and flowpaths followed mapable fill and spill locations based on 2 m resolution digital topographic analysis. Interestingly, while surface topography is relatively unimportant under unfrozen conditions at our site because of low relief and high infiltrability, surface topography shows episodically critical importance for connectivity and runoff generation when the ground is frozen.

1. Introduction

Understanding snowmelt-runoff generation in snow-dominated regions is critical for predicting water delivery and availability as the climate changes and these cold regions warm. While point-scale (*e.g.* Granger et al., 1984; Zhao and Gray, 1999) and hillslope-scale (*e.g.* Kane et al., 1981; Quinton and Marsh, 1999; Carey and Woo, 2001; Quinton et al., 2004; Suzuki et al., 2005) melt and runoff processes have been well studied, we still do not fully understand process controls on hillslope snowmelt-runoff connectivity – where, here 'connectivity' is conceptualised as the generation of continuous flow fields across a hillslope. Connecting point-scale runoff generation elements across hillslopes and catchments is now seen as fundamental for assessing the nonlinearities in runoff relations. Several studies have now shown how key nonlinearities like thresholds and feedbacks can produce emergent behaviour that is not explainable by traditional point-scale concepts (Grayson and Blöschl, 2001; Sivapalan, 2005; Bracken and Croke, 2007; James and Roulet, 2007; Troch et al., 2008; Ali and Roy, 2009; Bracken et al., 2013; McDonnell, 2013). In rainfall-runoff studies, pattern-based or spatially-distributed measurements have enhanced our understanding of hydrological connectivity and associated thresholds as linked to surface or bedrock topography (Darboux et al., 2002; Tromp-van Meerveld and McDonnell, 2006) and soil moisture (Western et al., 2001; Penna et al., 2011).

Spatially-distributed approaches have supported the concept of fill and spill (Spence and Woo, 2003; Tromp-van Meerveld and McDonnell, 2006) as a potential underlying mechanism for emergent behaviour in runoff generation (McDonnell, 2013). The fill and spill mechanism posits that storage capacities (*e.g.* depressions) in subsurface or surface topography must fill to a certain threshold (*e.g.* the downslope sill of the depression) before it can spill downslope. Fill and spill has been used to account for: runoff

* Corresponding author.
E-mail address: anna.coles@usask.ca (A.E. Coles).
[1] Now at Wilfrid Laurier University, 5007 50th Avenue, Yellowknife, NT X1A 2P8, Canada.

https://doi.org/10.1016/j.jhydrol.2018.01.016
0022-1694/

from soil-filled valleys in which valley physiography has created segments of varying storage conditions (Spence and Woo, 2003); subsurface stormflow at the soil-bedrock interface on forested hillslopes (Tromp-van Meerveld and McDonnell, 2006; Hopp and McDonnell, 2009); and subsurface stormflow above an argillic zone on low-relief forested hillslopes (Du et al., 2016; Jackson et al., 2016). In peat-dominated, permafrost environments, filling and spilling of spatially variable storage above a frost table has been shown to generate hillslope subsurface flow (Wright et al., 2009) and surface runoff connectivity (Williams et al., 2013). Catchment-scale overland flow generation analogous to fill and spill has been observed in lake--dominated landscapes (Leibowitz and Vining, 2003; Shaw et al., 2012; Leibowitz et al., 2016). Surface overland flow studies at the hillslope scale have shown that runoff is modulated by micro-topography and surface roughness (Darboux et al., 2002; Appels et al., 2011; Chu et al., 2013). While not labelled *sensu stricto* as 'fill and spill', they too are examples of overland flow being driven by the filling and spilling of depressions at a partitioning surface with loss along the flowpath and emergent runoff behaviour at the larger scale (Ameli et al., 2015).

The fill and spill mechanism fits within a storage-excess framework of water delivery (Spence, 2010; McDonnell, 2013). Existing runoff concepts are limited in geographic relevance; for example, the variable source area theory (Hewlett and Hibbert, 1967) typically only explains runoff generation in humid, vegetated sites, while the partial area concept (Betson, 1964) is restricted to arid or infiltration-excess overland flow systems (McDonnell, 2013). While fill and spill is not a theory *per se*, McDonnell (2013) suggested that it represents a framework that could describe the storages and connectivity relationships for a given site, and lead to new theory linking the similarities of runoff processes – one that is related to storage, storage thresholds, and connectivity (Spence, 2010).

Although evidence now abounds linking storage exceedance and emergent runoff behaviour with the fill and spill mechanism, relatively few studies have observed such a mechanism in frozen environments (Spence and Woo, 2003; Wright et al., 2009; Williams et al., 2013). No studies that we are aware of have examined whether or not such a mechanism operates over seasonally-frozen ground on the well-drained, glacial deposits of the northern Great Plains of North America. Melt onto frozen ground is notoriously difficult to model (Gupta and Sorooshian, 1997; Pomeroy et al., 2007). On the northern Great Plains, this is especially difficult due to minimal topographic slope and deep, permeable soils. Upscaling point-scale frozen ground runoff measurements (*e.g.* Granger et al., 1984; Zhao and Gray, 1999) to the hillslope scale has been difficult. For instance, Coles (2017) tested the widely-used infiltration model of Granger et al. (1984) over 52 years of snowmelt-runoff recorded at the Swift Current hillslopes in Saskatchewan and found that the point-scale model explained only 13.6% of the hillslope-scale runoff ratio.

Runoff in the melt season on the northern Great Plains is typically infiltration-excess overland flow over frozen ground (Fang et al., 2007). Natural drainage systems at the landscape scale are poorly developed, disconnected and sparse, due to the aridity and exceptionally low angled topography (Fang et al., 2007). During the snowmelt season, a third of the annual precipitation melts within 1–2 weeks to generate *c.* 80% of the annual runoff. At the hillslope scale we might expect that these factors encourage sheet-like overland flow across the soil surface. At the same time, shallow slopes and a poorly-defined drainage system can lead to a large non-contributing proportion of a hillslope. This is observed at larger basin scales in these regions, where large non-contributing areas exist even under extremely wet conditions (Stichling and Blackwell, 1957; Martin et al., 1983).

While undulations in the frozen soil surface could be enough for the occurrence of spatial flowpath organization and/or non-contributing areas, these need to be mapped and addressed. Critically too, the contrast between frozen ground infiltrability and snowmelt input rates dictate whether or not overland flow is generated– these are rarely mapped or reported. If the contrast is large enough, it may enable widespread filling and spilling and whole-hillslope connectivity. If the contrast is too small (less than 10^1 as noted by Hopp and McDonnell (2009) and James et al. (2010)), it would encourage infiltration, loss along a flowpath, and diminished or negated connectivity.

When frozen, a soil's infiltrability is usually less than its unfrozen state (Granger et al., 1984), but frozen infiltrabilities are varied and can sometimes still be considerable (Burt and Williams, 1976), especially in low soil moisture conditions. For example, Spence and Woo (2003) observed infiltration rates of 41 mm hr^{-1} on the subarctic Canadian Shield regardless of the frozen state of the unsaturated soil. Fang et al. (2007) observed greater infiltration than runoff on frozen, agricultural fields in southern Saskatchewan due to dry soils from the previous year's cropping. Zheng et al. (2001) found that cumulative infiltration into thawed soil (65.6 mm) was only 19.1% greater than infiltration into shallow frozen soils (55.1 mm). Snowmelt rates, too, are highly variable. Spence and Woo (2003) noted that melt input intensity averaged 0.11 mm hr^{-1} and melt water readily infiltrated their relatively high-infiltrability frozen soils. At the Swift Current hillslopes, season-averaged snowmelt rates over a 52-year period have varied between 0.39 and 4.63 mm hr^{-1} (Coles, 2017).

Here we explore the factors controlling the patterns and mechanisms of hillslope meltwater runoff on seasonally-frozen ground of the northern Great Plains, specifically at the Swift Current hillslopes in southwest Saskatchewan. We build upon long term analysis at this site (Coles, 2017) but focus on the 2014 melt season. We measure the spatial patterns of snow cover, snow water equivalent, soil water content, thawed layer depth at the soil surface, and surface topography to understand the primary controls and processes behind hillslope-scale runoff activation. We seek to understand the role of micro-, meso-, and macro-topographic features in controlling the snowmelt-runoff response and explore the similarities and differences in comparison to warmer and/or more steeply sloping regions (*e.g.* Darboux et al., 2002; Appels et al., 2011; Chu et al., 2013; Tromp-van Meerveld and McDonnell, 2006). We combine these hydrometric observations and mapping of spatial patterns with isotope analysis of snowmelt inputs and runoff outputs to mechanistically assess snowmelt-runoff over frozen ground. Specifically, we address the questions:

i. How do hydrological and structural spatial patterns – those of snow cover, snow water equivalent, soil water content, thawed layer depth, and surface topography – dictate connectivity and hillslope runoff generation over frozen ground?
ii. Are the controls on connectivity consistent with the fill and spill mechanism found elsewhere?

2. Study site

The Swift Current hillslopes are three adjacent agricultural hillslopes located at South Farm, Swift Current (50°15′53″N 107°43′53″W) in southern Saskatchewan in the Canadian Prairie region of the northern Great Plains. We focus our high resolution spatial analysis on Hillslope 2 (Fig. 1), - with an area of 46,600 m^2. A raised, grassed berm around the perimeter of the hillslope prevents surface water entering from adjacent land and ensures that the only outlet for runoff is an instrumented H-flume at the

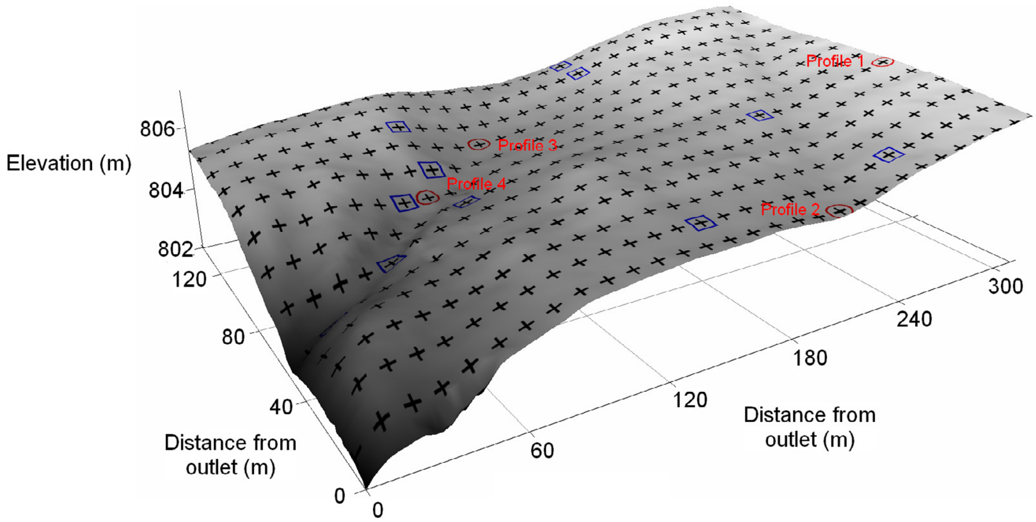

Fig. 1. Digital elevation model of the surface topography of Hillslope 2, with vertical exaggeration. Also shown: 10 × 10 m measurement grid (plus signs), locations of the four soil moisture and soil temperature profiles (red circles), and locations of the 11 snowmelt lysimeters (blue squares). North is at left. The only surface runoff outlet from the hillslope is at point (0,0).

hillslope's northwest corner (point (0,0) in Fig. 1). The hillslope is slightly concave in shape, has gradients of 1% in the upper two-thirds of the hillslope and 2.5% in the lower one-third, and slopes towards the northwest. A digital elevation model (DEM), obtained using a Leica Viva GS15, for the hillslope has a 2 m horizontal resolution and a 0.015 m vertical resolution. At a finer scale than the 2 m horizontal resolution are micro-topographic features – ridges and furrows – from seeding the hillslope. If the ground is not tilled following harvest, these features remain through the winter and into the spring. This was the case in the spring of 2014, the season studied here. The hillslope was ploughed and seeded in early summer 2013 in a north-south direction, with wheat planted in the raised ridges (*c.* 5–15 cm in elevation above the furrows, and the cross-section of one ridge and one furrow being approximately 30–50 cm wide).

The soil is a Swinton silt loam and classified as an Orthic Brown Chernozem (Cessna et al., 2013). Data from a one-location soil profile investigation, with measurements taken at 15 cm intervals from 0 to 180 cm below the soil surface, were provided by Agriculture and Agri-food Canada. Silt content decreases with depth from 50.4% in the 0–15 cm surface layer to 27.9% at 150–165 cm, clay content increases with depth from 18.2% to 30.9%, and sand content fluctuates between 24.4% and 42.4% through the profile. There is a clay layer (48.4% clay) observed at a depth of 165–180 cm (which presumably prevented deeper investigations). The general soil type is silt loam for the upper 60 cm of the soil profile, and clay loam beneath this. Bulk density increases with depth, from 1.22 g cm^{-3} at 0–15 cm to 1.59 g cm^{-3} at 120–135 cm, below which it decreases to 1.43 g cm^{-3}. Observations also show that saturated hydraulic conductivity increases with depth: from 1.42 cm hr^{-1} at 0–15 cm to 5.76 cm hr^{-1} at 75–90 cm (no data deeper than 90 cm).

We characterized the spatial variability of soil depth and surface infiltration capacity in July-August 2013. Soil probing with a dynamic cone penetrometer (Shanley et al., 2003) at 17 random locations on the hillslope showed the mean soil depth to be 265 cm (standard deviation = 45.3 cm). We used soil penetration resistance, measured by the penetrometer, as a proxy for soil permeability (Shanley et al., 2003), where higher resistance indicated lower permeability. Permeability patterns were relatively uniform in space for the upper 200 cm of the soil profile, but decreased with depth below 200 cm. In most of the 17 profiles, resistance increased, and thus permeability decreased, sharply at approximately 15–20 cm depth, for a layer approximately 5–10 cm thick. Another layer of low permeability (of varying thickness between 5 and 20 cm) was observed in most profiles between approximately 60–100 cm below the soil surface. A third, thin (*c.* 5–10 cm thick) layer of low permeability exists in some of the profiles between 120 and 200 cm below the soil surface, which likely reflects the clay layer identified in the archived soil profile data. Infiltration capacity measurements were undertaken with a constant head sprinkler infiltrometer at 62 random locations on Hillslope 2 (Seifert, 2014). They show unfrozen infiltration capacities to range between 0.4 and 63.5 mm hr^{-1}, with a mean of 13.9 mm hr^{-1} and standard deviation of 13.2 mm hr^{-1} (Seifert, 2014). Laboratory-based tests indicate that frozen surface infiltration capacities at this site are much lower, with a range between 0.09 and 2.57 mm hr^{-1}, and a median of 0.33 mm hr^{-1}.

Hillslope 2 typically is under an annual rotation of wheat (*Triticum aestivum* L.) and fallow, but with some instances in the last 52 years of grass (*Psathyrostachys juncea* (Fisch.) Nevski), lentils (*Lens culinaris* L.), and peas (*Pisum sativum* L.). Hillslope 2 has undergone both conventional tillage and zero tillage practices. In 2013, the year prior to our field campaign in spring 2014, Hillslope 2 was cropped with wheat and had been under zero tillage management. As a result, from September 2013 to May 2014 (encompassing the snowmelt period studied here, which had a duration of 12 days, from 9th to 20th March 2014) Hillslope 2 had standing wheat stubble residue with height of 30–50 cm. Precipitation data (measured using a Belfort weighing gauge) for the period of study were available from a nearby (*c.* 700 m to the south-southeast) Environment and Climate Change Canada standard meteorological station.

3. Methods

We used digital topographic analysis, specifically the calculation of two metrics (flow accumulation and downslope index), to develop a theoretical map of fill and spill locations across Hillslope 2. We then conducted high spatial and temporal resolution measurements of key hydrometric variables to explore changing spatial patterns of runoff production source areas. We combined high-frequency monitoring of runoff rates at the hillslope outlet with stable water isotope analysis of the runoff, snowmelt, and soil water, and with the hydrometric spatial maps to understand the drivers of connectivity and water delivery during the snowmelt season. We used the map of fill and spill locations to assess whether our field observations of the controls on connectivity were consistent with the fill and spill mechanism. These steps are outlined in greater detail in the following subsections.

3.1. Digital topographic analysis

Following Hopp and McDonnell (2009), we calculated two metrics – flow accumulation (FA) and downslope index (DI) – for each cell of the 2 m DEM. FA indicated the upslope contributing area of each cell, calculated as the number of cells upslope that drained into each cell. This was determined using the D8 flow algorithm, a common tool to determine the weighting of flow from each cell into the eight adjacent cells (Jenson and Domingue, 1988). The FA also indicates local topographic highs (ridges or sills), which are assigned an FA of 0.

DI indicated the downslope drainage efficiency of each cell. It was expressed as DI = V/H, where H is the horizontal distance that must be traversed in the steepest downslope direction to descend to a point at a pre-defined vertical distance (V) from the elevation of the starting cell (Hjerdt et al., 2004). While the DI was initially used to capture near-surface groundwater levels and 'backing-up', it is thought to be a useful tool in different terrains where topographic curvature controls local drainage regimes (Hjerdt et al., 2004). We used a V of 15 cm, selected because it is the maximum elevation change between a ridge and furrow. This ensures that any sporadic instances of a ridge or furrow being picked up in the 2 m horizontal resolution DEM are smoothed out from this topographic analysis. A cell with a small DI was caused by a long horizontal distance (H) and indicates that drainage from that cell was slow and inefficient (Tromp-van Meerveld and McDonnell, 2006; Hopp and McDonnell, 2009).

We used the combination of FA and DI to indicate potential fill and spill locations across the hillslope (Hopp and McDonnell, 2009). Locations with a large FA and small DI (shallow, long slopes with a large upslope contributing area) are typical of fill locations – areas where water can be collected and retained. Meanwhile, locations with a large FA and large DI (steep, short slopes with a large upslope contributing area) are typical of spill locations – areas where water can accumulate and then be efficiently drained.

In order to map fill and spill locations across the hillslope, we determined threshold values of FA and DI to define 'large FA', 'large DI', and 'small DI'. First, we examined the sensitivity of these threshold values, and how they affected the spatial fill and spill results. Increasing the FA threshold value led to a reduction in the quantity of cells that were designated as fill or spill locations (an increase in the quantity of nullified cells). Changes to the DI threshold affected the pattern of fill or spill across the hillslope; for example, a high DI threshold meant spill locations – from which water is able to reach the hillslope outlet – were restricted to the base of the hillslope, while a lower DI threshold created spill locations in all reaches of the hillslope.

We decided upon a FA threshold value of 10 m^2 and a DI threshold value of 0.015. The FA threshold value was decided upon following field observations during snowmelt of the percentage coverage of the hillslope that showed water at the soil surface: approximately one-third (further described in Section 3.2). This coverage was replicated with an FA threshold value of 10 m^2, which caused 29.8% of the hillslope to be designated as either a fill location or a spill location. The DI threshold chosen (0.015) was relatively low so that the potential importance of the small-scale (micro- and meso-) topographic relief could be captured (a high DI would be too coarse for these topographic nuances on low-angled terrain). Fill locations were designated when cells had FA > 10 m^2 and DI < 0.015. Spill locations were designated when cells had FA > 10 m^2 and DI > 0.015.

3.2. Hydrometric field measurements

We measured volumetric soil water content at 0–6 cm depth on a 480-point grid (a 10 × 10 m spatial resolution; Fig. 1) during several daily field campaigns (19th July 2013, 2nd August 2013, 9th August 2013, 3rd September 2013, 23rd September 2013, 24th October 2013, 28th March 2014, 7th April 2014, 13th May 2014, and 19th June 2014) using a portable Stevens HydraProbe POGO. Snow cover and frozen ground prevented these measurements being taken over winter. Therefore, the last soil water content mapping prior to freeze-up (24th October 2013) was used to capture the spatial variability in soil water content at the onset of frozen conditions. Mapping resumed on 28th March 2014 once there was no longer snow cover and the soil was thawed sufficiently for the probe to be inserted. For each survey, we made further soil water content measurements at smaller spatial resolution, within random 10 × 10 m grid squares, for geostatistical analysis. Variogram analysis following the first soil water content survey (19th July 2013) showed that the variance of the data stabilized at approximately 80 m, giving us confidence that a 10 × 10 m spatial resolution adequately captured the variability and spatial patterns.

We measured volumetric soil water content and temperature at five depths (sensing depth coverages of 0–6, 6–9, 21–24, 43.5–46.5, and 73.5–76.5 cm, with mid-points at 3, 7.5, 22.5, 45, and 75 cm, respectively) at four locations using Stevens HydraProbes. Each location was representative of a key landscape unit– upland area (Profile 1), two surface depressions (Profiles 2 and 3), and a slope (Profile 4) (Fig. 1). These measurements were logged at 30 min intervals for a period of 12 months (October 2013 to September 2014). Only soil water content data for periods when the soil temperature was >0 °C is useful here because the sensors determine soil water content via dielectric permittivity, which is not applicable to water content quantification in frozen, freezing, or thawing soils without considerable uncertainty (Williamson, 2016). We used data from 24th October 2013 and 24th April 2014 to assess the change in soil water content from pre-freeze up to post-melt, respectively.

We measured snow depth, and calculated density and snow water equivalent (SWE), on a 225-point grid (10 × 20 m spatial resolution in the lower two-thirds of the hillslope, and 10 × 40 m spatial resolution in the upper third) by manual snow surveys. These snow surveys were conducted several times through the winter (irregularly spaced and independent of snowfall occurrence) and just prior to the onset of snowmelt (timing depended on our expectation of when snowmelt would commence, which was based upon local air temperature forecasts and observations of snowpack temperature), and then daily, every morning before any significant melt, through the snowmelt period (9th March – 20th March 2014). We applied the following equation to calculate daily ablation at each of the 225 measurement points:

$$ablation_{day(x)} = SWE_{day(x)} - SWE_{day(x+1)} \tag{1}$$

where, $ablation_{day(x)}$ is the total snowpack ablation that occurred on a given day, x. It is calculated as the difference between the snow water equivalent (SWE) of the snowpack determined at that point on the morning of day x and the equivalent determined at that point on the morning of the following day $(x+1)$. The hillslope-average daily snowpack ablation is the mean of the daily ablation at the 225 points.

During the daily snow surveys, we noted any observations of water at the soil surface (visible only when a snow core was removed from the snowpack for measurement) to understand approximately the areal coverage of water at the soil surface. This coverage was used to define the FA threshold value (we referred to this in Section 3.1). We also measured snowmelt rate from the base of the snowpack manually using 18 snowmelt lysimeters at 11 locations (1–3 duplicates at some locations) at irregular time intervals (10–120 min) depending on melt rate (Fig. 1).

We measured surface thawed layer depth (depth to the top of the frozen ground) daily on a 60-point grid (20 × 40 m spatial resolution) by manually knocking in a length of 11 mm diameter rebar until frozen ground resistance was detected. This was always undertaken by the same researcher for consistency. This was also carried out at 2 h intervals at three locations to capture sub-daily changes in thawed layer depths.

Seven time-lapse standard-image cameras (Wingscapes) captured snow cover accumulation and ablation, and were used with personal observations to chronicle the snow-covered area, and locations of flowpaths and ponded water on the hillslope. Finally, runoff from the hillslope was logged at 15 min intervals through the snowmelt period using a pressure transducer (HOBO U20 Water Level Data Logger) in the stilling well of an H-flume at the outlet of the hillslope.

3.3. Isotope sample collection and analysis

Stable isotope analysis of water is one more tool that we employed to understand the mechanism of hillslope-scale runoff generation during the melt season. We used it to determine the ratio of 'new' snowmelt water to displaced 'old' soil water in the runoff. During the 2014 snowmelt season, we collected 1422 water, soil, and snow samples. These samples consisted of:

- 308 runoff samples from the flume at the outlet of Hillslope 2, collected using an ISCO 3700 which automatically sampled water flowing through the flume at 30 min intervals (15 min intervals during peak flow).
- 454 snowmelt samples from the base of the snowpack, manually extracted from each of the 18 snowmelt lysimeters, and taken at irregular intervals (10–120 min) depending on melt rate (*i.e.* the approximate length of time it took to obtain a full 25 ml sample vial of water).
- 50 soil samples, collected prior to snowmelt on 20th February 2014 from two depths (0–6 cm and 6–15 cm) at 32 locations on Hillslope 2 using a slide-hammer corer. These were taken to obtain pre-event soil water, which, along with the snowmelt water, is an important potential end-member in the runoff signature.
- 217 snow core and incremental snow samples, collected during the snow survey, melted down and bottled.
- 63 ponded water (on the soil surface or snow surface) samples, collected several times per day from any areas of ponded water.

All bottled water samples were sealed and stored in a non-refrigerated, cool and dry location. The soil samples were double-bagged and kept frozen until it was possible to extract their soil water. We extracted the soil water by high pressure mechanical squeezing (Orlowski et al., 2016). The isotopic compositions of the liquid water samples were then determined by analysis on a Liquid Water Isotope Analyzer (Los Gatos Research) and reported in parts per thousand (‰) relative to VSMOW (Vienna Standard Mean Ocean Water), a standard of known composition.

3.4. Spatial patterns mapping

For all sets of data for each spatially-measured variable (surface soil water content, depth of thawed layer, and snow cover ablation), we interpolated the data points using kriging (Sarma, 2009) to provide gridded data for each variable at exactly the same points. We used ordinary point kriging with a linear variogram model to weight the surrounding measured values to derive a predicted value for an unmeasured location. Only the data of the variable of interest were considered in the interpolation, while other factors such as elevation and spatial heterogeneities of soil properties that might influence the spatial patterning of the data were not considered in the interpolation process. This might affect the interpolation accuracy. We employed cross-validation using all measured values to determine the quality of the gridded data. Maps were generated from the kriged datasets.

4. Results

4.1. Digital topographic analysis

To understand the potential effects of topographic features (Fig. 2a) on surface runoff from Hillslope 2, we assessed the combination of the flow accumulation (FA) and downslope index (DI) metrics as an indicator of potential fill and spill locations across the hillslope. FA exhibits a power law distribution, whereby a histogram of the data extends from 0 to 4000 m^2 with the majority of the cells having a FA < 20 m^2 and a long tail of data from 20 to 4000 m^2. We truncated the mapping of FA to <100 m^2. The FA map (Fig. 2b) shows that individual flowpaths with higher FA are distributed across the whole hillslope. There are five flowpath systems, all draining in a northwest direction towards the hillslope outlet. Two drain the lower third (2.5% slope) of the hillslope, and three drain the upper two-thirds (1% slope). Flowpath system 1 is connected to the outlet by a thin flowpath on the upper west (left) border of the hillslope. However, flowpath systems 2, 3, 4, and 5 do not appear to be connected directly to the outlet: all four are separated from the outlet by cells of lower (lighter) flow accumulation, and also by the flowpath systems downslope (flowpath system 5 drains through 3 and then 1; while flowpath system 4 drains through 2 and then 1). Any surface ponding or retention of water would occur at the mouths of these individual systems. We calculated the area and volume of depressions on the hillslopes using the "Fill" tool in ArcMap 10.2. This highlighted five areas of ponding, in line with the above analysis, at the mouths of the individual drainage systems (Table 1).

The raised grass berms also influenced water ponding at the mouths of flowpath systems 2, 3, and 5. The raised grass border on the west side of the hillslope impedes water that is flowing towards the northwest from flowpath systems 3 and 5, causing it to pond between the raised border and a natural topographic sill on the hillslope. Downslope of the mouths of flowpath systems 3 and 5, the western raised grass border acts as a funnel for runoff down the western side. Similarly, the northern raised grass border impedes flow in the northerly direction from flowpath system 2, and also acts as a conduit for flow towards the hillslope outlet along the hillslope's northern edge.

The DI map (Fig. 2c) indicates that the majority of the hillslope, especially the upper two-thirds, has a low DI and therefore a low drainage efficiency. An area of high DI and therefore high drainage efficiency exists in the lower third of the hillslope and reflects the valley-like surface topography (Fig. 2a). Combining FA and DI indicates the balance of fill and spill across the hillslope (Fig. 2d). 29.8% of the hillslope is designated as either a fill location or a spill location. The majority (57.4%) of the designated cells are fill locations, with these concentrated in the upper two-thirds of the hillslope. The spill locations (42.6%) are primarily in the lower third of the hillslope, but there are a limited number of small spill locations in the upper third of the plot also. Fill locations appear to be relatively well connected to one another, especially in the central third of the hillslope, and are fed by spill locations further upslope. The fill locations are set back from the hillslope outlet, with a swath of spill locations in the intervening area. This suggests that once the

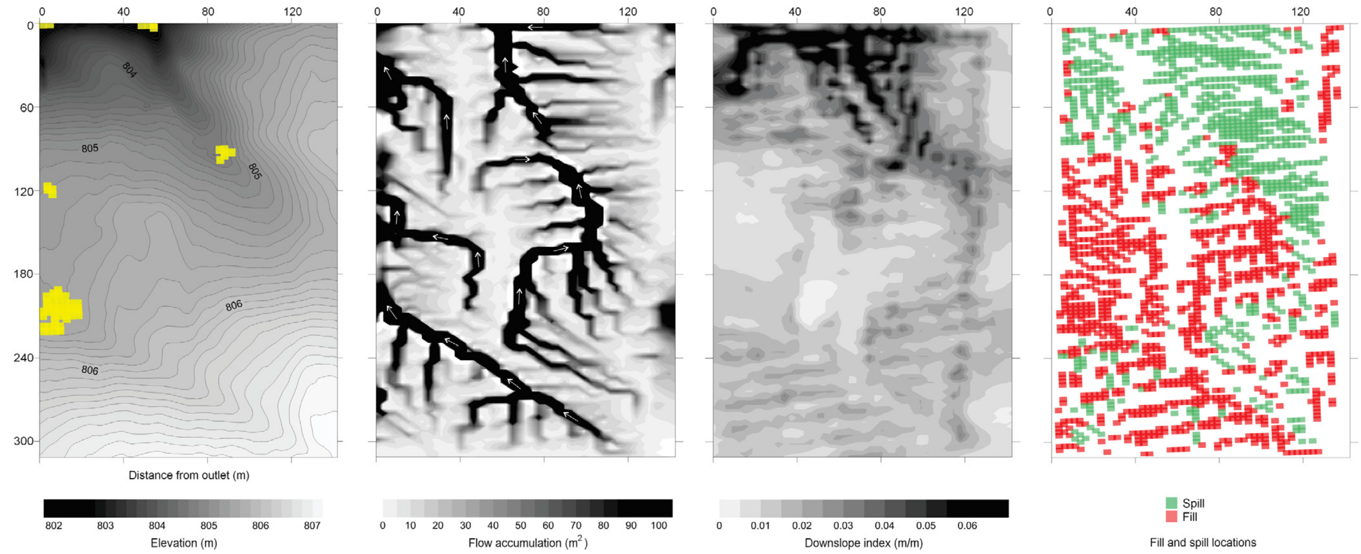

Fig. 2. Maps of (A) the DEM of the surface topography, as in Fig. 1, highlighting in yellow the locations of surface depressions detailed in Table 1; (B) flow accumulation (FA), with five sub-hillslope flowpath systems identified (drainage systems 1–5) and the general flow directions indicated by the arrows; (C) downslope index (DI); and (D) fill and spill locations, where fill locations are defined as having FA > 10 m^2 and DI < 0.015, and spill locations are defined as having FA > 10 m^2 and DI > 0.015. North is at top.

Table 1
Area, depth (mean and maximum), and volume of depressions at the mouths of each flowpath system.

Location of depression	Area (m^2)	Depth (m)		Volume (m^3)
		Mean	Maximum	
Mouth of System 1	18	0.0775	0.128	1.40
Mouth of System 2	54	0.0328	0.0564	1.77
Mouth of System 3	27	0.0716	0.113	1.93
Mouth of System 4	45	0.0210	0.0499	0.943
Mouth of System 5	324	0.0593	0.140	19.2

fill locations – in the upper two-thirds – spill, due to water input exceeding the surface detention storage capacity, the released water can be efficiently routed through the spill locations – over the lower third – and to the hillslope outlet. Not captured by the DEM or topographic analysis are the micro-topographic ridges and furrows.

4.2. Hydrometric analysis

4.2.1. Snowmelt, snow cover, and runoff

The 2014 melt season had high total winter snowfall (77.5 mm SWE, between 1st October 2013 and 31st March 2014), a large snow cover (78 mm SWE), and a low-medium runoff amount (25 mm). The 78 mm SWE of the snow cover melted over 12 days, between 9th March 2014 and 20th March 2014, with peak snowmelt on 16th March (Fig. 3a). Runoff from the hillslope began on 12th March and finished on 20th March, with peak runoff occurring in concert with peak snowmelt on 16th March (Fig. 3a,b). Peak runoff rate on 16th March was 11.6 times greater than the peak runoff rate on the previous day. The instantaneous increase in runoff after hillslope-wide connectivity was achieved at 15:00 on 16th March was 7.2 times greater than just before connectivity was achieved (13:45 on 16th March). There were four evolving stages (Fig. 3) of meltwater inputs to the soil surface and runoff outputs from the hillslope: Stage 1 (9th–12th March): initial snowmelt, but no resulting hillslope runoff; Stage 2 (13th–15th March): continued snowmelt, with moderate hillslope runoff; Stage 3 (16th March): high volumes of snowmelt and high runoff; Stage 4 (17th–19th March): low snowmelt and small amounts of runoff.

The spatial patterns of snow cover ablation (Fig. 3c) indicate that snowmelt occurred unevenly over the hillslope, with concentrated patches of snowmelt that changed in location over time. Daily snow cover ablation ranged between 0 and 70 mm over the hillslope. Sub-daily measurements at snowmelt lysimeters across the hillslope showed that, at its peak on the afternoon of 16th March, snowmelt occurred at 1.17–8.21 mm hr^{-1}. We observed water ponding in the bottoms of the micro-topographic furrows at the soil-snow interface, with flow along these features in the downslope direction. Maximum water movement was in the mid-afternoons, when some snowmelt lysimeters would become overwhelmed (and subsequently abandoned) by water flowing in from upslope. From 11th to 16th March, larger areas of ponded water gradually accumulated along the western edge of the hillslope (Fig. 3d) (at the mouth of flowpath system 3 and 5), at the top of the valley-like system (at the mouth of flowpath system 4), and at the northern edge of the hillslope (at the mouth of flowpath system 2). Ponded water was at its maximum on 16th March, and decreased in extent over the following days.

Fig. 4 shows the snow cover ablation and development of ponded water on the western edge of the hillslope. Snow-covered area remained high over the hillslopes throughout most of the melt season, falling gradually from 100% on 11th March to 90.7% on 15th March, to 75.8% on 16th March (the day of peak melt and runoff), and then rapidly decreasing to 20.5% on 20th March. After 20th March, a small amount of snow remained on the hillslope at the northern edge of the hillslope, which took a further 6 days to clear.

4.2.2. Thawed layer depth

The ground was frozen to the soil surface homogenously across the hillslope, in the initial melt days, and during peak melt and runoff (16th March) (Fig. 5a). Following peak runoff, the thawed layer deepened rapidly and unevenly (Fig. 5b). On 18th March, the ground had thawed to depths of 15–20 cm below the soil surface, but only in isolated patches across the hillslope: most notably, on the upland at the south end of the hillslope, and on a southwest-facing slope in the valley-like feature at the base of the hillslope. The ground remained frozen to the soil surface where snow cover remained.

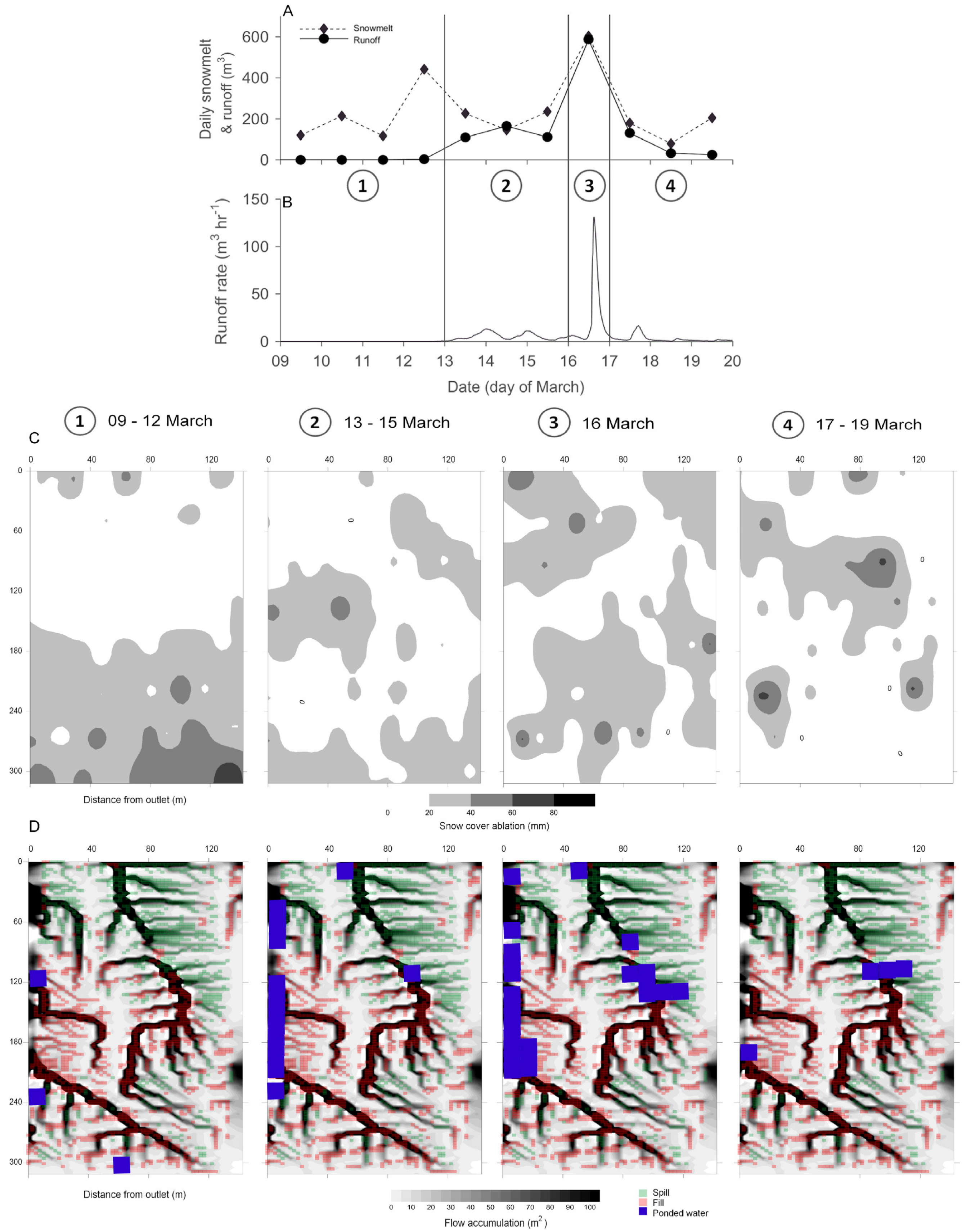

Fig. 3. For the 2014 spring snowmelt season on Hillslope 2: (A) daily snowmelt and runoff volumes and (B) runoff rates, recorded at 15-min intervals. Four stages (1–4) are identified in the snowmelt-runoff, referred to in the text. Maps relate to each of these stages: (C) snowmelt over the hillslope for each stage; and (D) ponded water locations during each stage overlaid on fill and spill locations and the flow accumulation map.

Fig. 4. Time-lapse photographs from the west side of Hillslope 2, facing northeast, showing the snow cover ablation and development of ponded water at the mouth of flowpath system 5.

4.2.3. Soil water content

The 2014 melt season was preceded by a dry autumn in 2013. On average, the soil water content in the surface 0–6 cm layer was 0.15 (from the 24th October 2013 survey). We found that surface soil water content on 24th October 2013 (Fig. 6a) showed relatively limited spatial variability, typical of all soil water content surveys conducted (Fig. 6b). We can therefore assume that the soil water content at the onset of snowmelt was relatively spatially homogeneous. Further, because of long soil moisture memory in this frozen, dormant system (Coles, 2017), the pre-freeze up soil water content (Fig. 6a) is likely representative of soil water content at the onset of the 2014 snowmelt season.

Soil water content generally increased following snowmelt under all four main landscape units (Profiles 1–4) (Table 2.

). The soil water content change was highly spatially variable. The soil profile situated in the shallow sloping, upland region of the hillslope (Profile 1) had the smallest increase in soil water content, with a net increase of 8.67 mm added to the profile (with gains close to the soil surface, but losses at depth). This profile location is representative of the majority of the hillslope. By comparison, soil profiles situated in the depressions (Profile 2 and 3, at the mouths of flowpath systems 5 and 4, respectively) saw net increases of 80.3 mm and 121 mm, respectively. Finally, the soil profile on the slope (Fig. 4), in the valley-like topography saw a net increase of 148 mm of soil water. Weighting the soil profile's water content change by their representative area suggests a hillslope-wide recharge of 0–90 cm soil water of 25 mm.

4.3. Isotope analysis

Stable water isotope analysis shows that the $\delta^{18}O$ and $\delta^{2}H$ of runoff water was largely temporally-constant (on average, runoff water $\delta^{18}O$ was -21.7 ± 0.742‰, and $\delta^{2}H$ was -169 ± 4.56‰), but with gradual enrichment of both isotopes through the melt season (Fig. 7). The isotope signatures of the snowmelt water (on average, snowmelt water $\delta^{18}O$ was -22.3 ± 2.10‰, and $\delta^{2}H$ was -171 ± 15.4‰) bounded the runoff water, albeit with a high amount of variability. By comparison, the pre-event soil water was much more enriched than the runoff water (on average, soil water $\delta^{18}O$ was -14.6 ± 1.97‰, and $\delta^{2}H$ was -128 ± 11.0‰). Two-component hydrograph separation using the mean $\delta^{18}O$ or mean $\delta^{2}H$ soil water values for the pre-event end member, and the mean $\delta^{18}O$ or mean $\delta^{2}H$ snowmelt values from each lysimeter for the event end member, showed that the runoff water is primarily composed of 'new' snowmelt water, with very little mixing with the pre-event 'old' soil water. Regardless of the isotope ($\delta^{18}O$ or $\delta^{2}H$) or lysimeter analyzed, hydrograph separation showed that the runoff water was composed of 100% new snowmelt water in the initial stages of the snowmelt season. On the day of peak runoff (16th March), runoff water was composed of on average 93.9% event snowmelt water. Towards the end of the snowmelt and runoff season, on 19th March, this value had declined to on average 67.6%. Through the entire season, runoff water was approximately 95.1% event snowmelt water and 4.9% pre-event soil water.

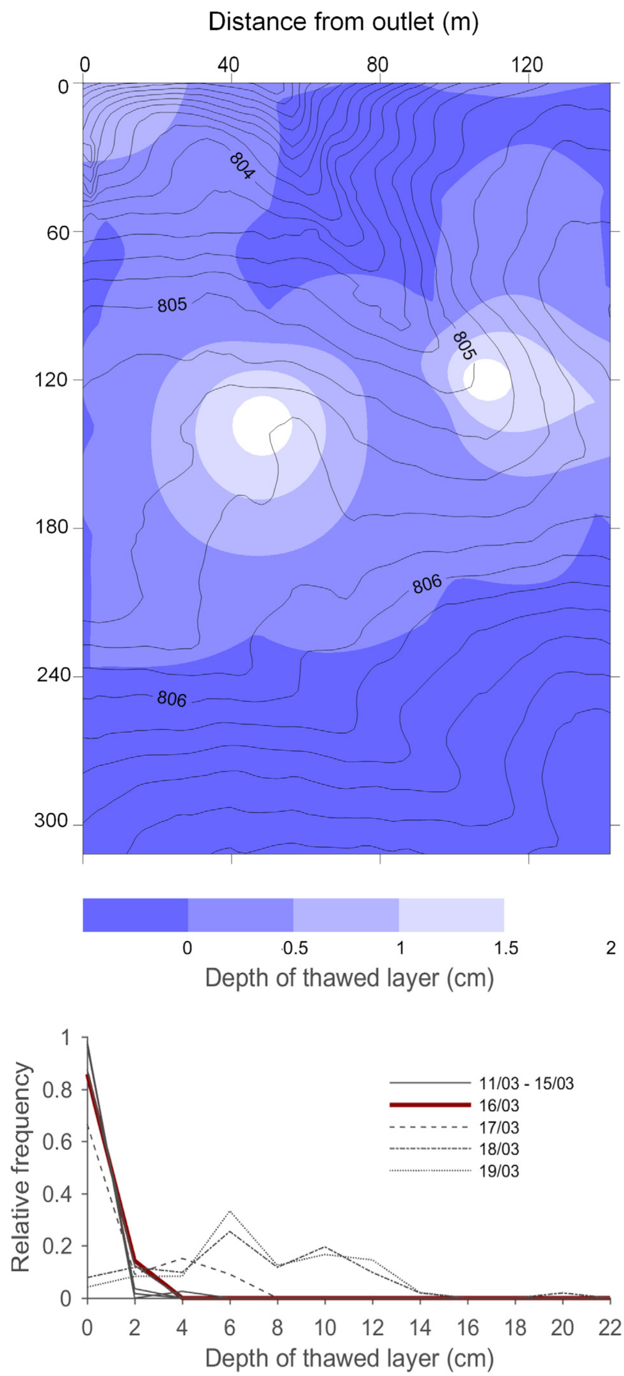

Fig. 5. (A) Spatial map of thawed layer depth on the day of peak snowmelt and peak runoff (16th March 2014); and (B) frequency distributions of all thawed layer depth surveys conducted, with 16th March 2014 survey highlighted in red. Note that the colour scale of the spatial map (A) is the same extent as the x-axis of the frequency distributions in (B).

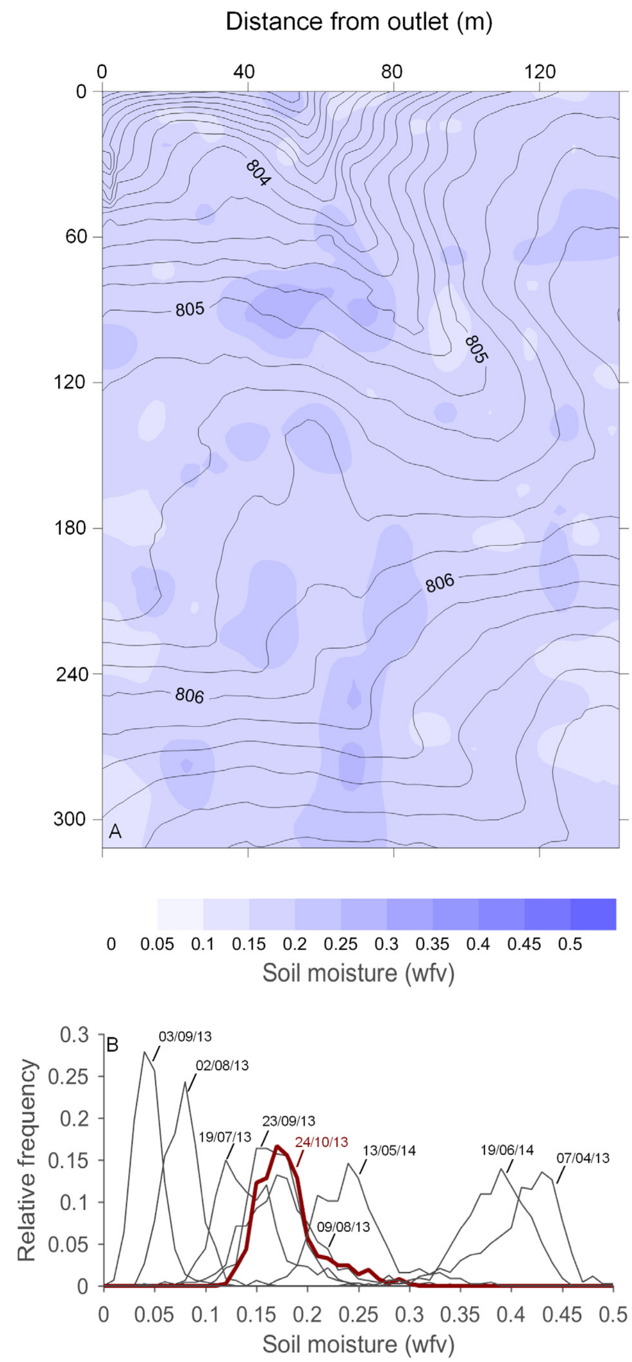

Fig. 6. (A) Spatial map of pre-freeze up soil surface water content (0–6 cm), measured on 24th October 2013; and (B) frequency distributions of all soil water content surveys conducted, with 24th October 2013 survey highlighted in red. Note that the colour scale of the spatial map (A) is the same extent as the x-axis of the frequency distributions in (B).

5. Discussion

Our results suggest that a mechanism analogous to fill and spill processes observed elsewhere explains the generation of snowmelt-runoff over frozen ground at our site. Our stable isotope analysis of meltwater confirmed that runoff water was 'event' snowmelt water with limited mixing with pre-event soil water. Unlike in steep terrain (*e.g.* Eriksson et al., 2013), lateral flow through the snowpack at our site was unimportant. The key factor generating fill and spill at our site is the large contrast between the low infiltration capacity of the uniformly and fully frozen soil surface and the relatively fast rates of snowmelt water delivery to the soil surface. This was enough to generate ribbons and ponds of water beneath the snow at the soil surface that accumulated in micro- and meso-topographic depressions, which then spilled downslope. Our observations of ponded water and flowpaths were consistent with mapped predictions of fill and spill activity from high resolution digital topographic analysis. We enunciate these features in the following sections.

Table 2
Pre-freeze (24th October 2013) and post-melt (24th April 2014) soil water contents at five depths at four key landscape units.

Soil profile	Depth interval (cm)	Pre-freeze soil water content		Post-melt soil water content		Change in water content (mm)
		vwc	mm	vwc	mm	
1 (upland)	0–6	0.134	8.04	0.182	10.9	2.88
	6–15	0.220	19.8	0.261	23.5	3.69
	15–30	0.167	25.1	0.193	29.0	3.90
	30–60	0.110	33.0	0.109	32.7	−0.300
	60–90	0.166	49.8	0.161	48.3	−1.50
2 (depression)	0–6	0.236	14.2	0.163	9.78	−4.38
	6–15	0.242	21.8	0.310	27.9	6.12
	15–30	0.224	33.6	0.316	47.4	13.8
	30–60	0.143	42.9	0.268	80.4	37.5
	60–90	0.144	43.2	0.235	70.5	27.3
3 (depression)	0–6	0.199	11.9	0.209	12.5	0.600
	6–15	0.207	18.6	0.316	28.4	9.81
	15–30	0.177	26.6	0.387	58.1	31.5
	30–60	0.150	45.0	0.319	95.7	50.7
	60–90	0.184	55.2	0.279	83.7	28.5
4 (slope)	0–6	0.196	11.8	0.266	16.0	4.20
	6–15	0.229	20.6	0.316	28.4	7.83
	15–30	0.158	23.7	0.339	50.9	27.2
	30–60	0.063	18.9	0.293	87.9	69.0
	60–90	0.070	21.0	0.202	60.6	39.6

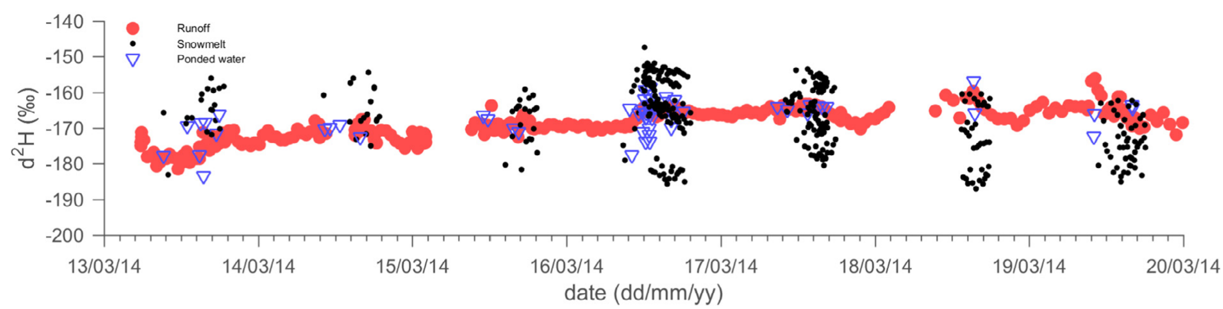

Fig. 7. Time series of stable isotopes (for $\delta\,^2H$) of runoff, snowmelt, and ponded water through the snowmelt season. Pre-event $\delta\,^2H$ soil water values measured on 20/02/14 (not shown) range between −112‰ and −140‰.

5.1. Micro-, meso-, and macro-scale topographic controls on fill and spill

Thawed layer depth data across the slope showed uniformly frozen soil to the soil surface (thawed layer depth = 0 cm) in the days leading up to, and during peak runoff. Frozen ground infiltration capacities have been observed at this site to range between 0.09 and 2.57 mm hr^{-1}, with a median of 0.33 mm hr^{-1}. Snowmelt rates during peak snowmelt in 2014 were 1.17–8.21 mm hr^{-1}. The relatively high rates of snowmelt water delivery to the soil surface largely exceeded the infiltration capacity of the frozen soil by a magnitude greater than 10^1, the hypothetical minimum contrast between bedrock and soil permeabilities required to generate runoff via the fill and spill mechanism at the soil-bedrock interface (Hopp and McDonnell, 2009). As such, we had an impeding layer contrast that was sufficient for the accumulation of water on the soil surface. This hints at the importance of soil temperature (whether a frozen, thawing or thawed state): if peak snowmelt had occurred on ground that was thawing or had thawed, connectivity and runoff likely would not have been triggered by the mechanism described here.

The concavity in the monitored hillslope is a macro-topographic feature (>10,000 m^2) of the site. The concavity affects the balance of fill and spill: the relatively steeper (2.5%) lower third of the hillslope was a dominant spill location. The flatter (1%) upper two-thirds was a dominant fill location. This pattern is a site-specific feature. Variations in hillslope shape would show altogether different fill-spill patterns. For example, a convex hillslope where the lower part of the hillslope is shallow, and the upper part more steep, would have a reverse fill-spill pattern to that observed here. Our terrain analysis indicated a balanced fill-spill regime with 57.4% of the hillslope characterized by 'fill' locations, and 42.6% by spill locations.

At finer scales, the *meso*-topographic features (100–10,000 m^2) revealed five flowpath systems in the flow accumulation (FA) mapping. Flowpath systems 1 and 2 drained the lower third of the hillslope; flowpath systems 3, 4, and 5 drained the upper two-thirds. These latter flowpath systems terminated at their downslope edges by slight 'lips' in the surface topography. These lips were enough to create a backwater effect and to create a fill region. We observed that the lips must be overcome for the upper region of the hillslope to connect to the lower, spill region of the hillslope and thus the hillslope outlet. The FA, DI, and fill and spill maps (Fig. 2), where these lips are visible, are useful tools to interpret the mechanisms behind ponding, storage exceedance, and rapid delivery of water. Important, though, is that each cell of these maps is solely an indicator of the local topographic surface. Additional research could seek to incorporate a metric for the likelihood of flow pathways being disconnected by a fill location created by a sill. Possible approaches to this could be to experiment with increased values of V (DI = V/H), which would then integrate topography further downslope from the starting point, or to use a metric of flowpath distance to the hillslope outlet and the fill locations it must overcome.

Nested within these macro- and meso-scale topographic systems, the micro-topographic features (<100 m^2) also exhibited a flow control during meltwater runoff. These small undulations were observable within the 10 $\times$ 10 m measurement grid. Most notably, these were ridges and furrows left behind from tractor-based seeding in the previous summer. While these micro-scale features were not visible in the 2 m DEM, they were an important localized feature in the initial routing and retention of melt water. Melt water pooled in, and was gradually routed downslope by, the furrows within each of the five flowpath systems. In flowpath systems 1 and 2, fill and spill occurred mainly within the furrows. In flowpath systems 3, 4, and 5, however, the routing of water via these furrows and small undulations was overtopped by ponded water that developed and grew in volume upslope from the lips, after which these barriers were overcome and water could spill over and coalesce at the hillslope outlet. Overall, the hillslope exhibited nested filling and macro-spilling.

Our finding that topography dictates hillslope-scale connectivity and snowmelt-runoff generation over frozen ground is in contrast to Devito et al. (2005). They examined a boreal plain site with more surficial geology variation, but importantly with similar low relief and deep glaciated substrate as the Swift Current hillslopes. Devito et al. (2005) dismissed the importance of surface topography. The key difference is that their evaluation was for a summer period when the ground was unfrozen and the deep, high-infiltrability mineral soils promoted vertical flow infiltration. Indeed, an analysis of summer rainfall-runoff events at our site would support the suggestion that topography is unimportant, since all water infiltrates except in exceptional storms (in only 28 years of the 52-year record have summer storms generated runoff; Coles, 2017). But critically, we see here that topography is episodically important during melt onto frozen ground. Topographic features acted as both a conduit for meltwater runoff (that enabled flowpath formation and connectivity once threshold surface detention levels were exceeded) and a loss mechanism (that enabled ponded water to form, and then heightened infiltration and soil water recharge under depressions when the ground started to thaw).

5.2. Fill and spill over shallow, frozen hillslopes in relation to other environments

The hydrologic response on Hillslope 2 of the Swift Current hillslopes reflected the fill and spill mechanism already observed in many other environments (Spence and Woo, 2003; Leibowitz and Vining, 2003; Tromp-van Meerveld and McDonnell, 2006; Wright et al., 2009; Graham and McDonnell, 2010; Appels et al., 2011; Du et al., 2016; Jackson et al., 2016; Leibowitz et al., 2016). The fill and spill mechanism was first introduced in a subarctic soil-filled valley with spatially-variable subsurface storage capacities, due to varying soil depths to bedrock, that had to fill up in order to enable surface runoff (Spence and Woo, 2003). The definition of the mechanism was further developed following analogous observations that showed depressions in subsurface or surface topography must fill up to a certain threshold (the downslope sill of the depression) before water can spill downslope (*e.g.* Tromp-van Meerveld and McDonnell, 2006; Leibowitz et al., 2016). These fill and spill observations fall within a storage-excess framework of water delivery (Spence, 2010; Sayama et al., 2011; McDonnell, 2013). The observations presented in this paper are fundamentally the same as those observations of fill and spill of depressions across an impeding layer, and of a storage-excess delivery of runoff.

The particular fill and spill mechanism described here is different to most previous observations, primarily because it is snowmelt over a frozen soil surface. This environment sees months of runoff inactivity with no whole-hillslope connectivity, and then 1–2 weeks where fill and spill over frozen ground delivers the large annual runoff pulse. This short, acute period of runoff occurs with the concurrent conditions of a frozen soil surface and high volumes of liquid water, as also described in Williams et al. (2013) for intermittent surface runoff connectivity over frozen peatland. This is unlike the humid, temperate regions where bedrock fill and spill is primed and relatively frequently produces subsurface stormflow (Tromp-van Meerveld and McDonnell, 2006; Graham and McDonnell, 2010; Du et al., 2016; Jackson et al., 2016).

The scale at which we have observed fill and spill is different to most previous studies. Observations of this mechanism have typically been at the plot or trenched hillslope scale (*e.g.* Tromp-van Meerveld and McDonnell, 2006; Wright et al., 2009; Graham and McDonnell, 2010; Du et al., 2016), at the small catchment-scale (Spence and Woo, 2003), and at the landscape scale (*e.g.* Leibowitz et al., 2016). The nested filling and spilling across scales at our hillslope site is essentially the next scale down from the wetland filling and spilling described for the prairie pothole region (Leibowitz and Vining, 2003; Shaw et al., 2012; Leibowitz et al., 2016). The hillslopes of the northern Great Plains deliver water to these wetlands, whose connectivity is in turn also dictated by fill and spill, albeit a fill and spill mechanism that is influenced and mediated by additional factors such as groundwater-surface water interactions (Brannen et al., 2015) and storage memory (Shook and Pomeroy, 2011).

Our study site is a low gradient end member (slope 1–2.5%) in the fill and spill literature. Our analysis indicated a fairly balanced fill-spill regime with 57.4% of the hillslope characterized by 'fill' locations, and 42.6% of the hillslope characterized by 'spill' locations. This is in contrast to previous studies with slightly steeper (yet still relatively shallow) slopes (7.2% slope in Hopp and McDonnell, 2009; and 6–12% slopes in Du et al., 2016) that exhibited fill-dominated regimes, which was attributed to their 'flatness'. As slope angle decreases, hillslopes appear to transition from a spill-dominated (on steep slopes) to a fill-spill balance (on medium slopes) and finally to a fill-dominated system (on shallow slopes) (Hopp and McDonnell, 2009; Reaney et al., 2014). Our fill-spill balance is perhaps more typical of medium-angled slopes. We attribute the difference between our fill-spill balance and these other low-angle studies' fill-dominated regimes to the difference in overall hillslope form. While these other studies' hillslopes were largely planar, ours is concave. The downslope barriers at the edge of the concave cross-section created the surface depressions that retained water and dictated upslope fill locations. Downslope of these barriers, any runoff at a point was able to flow unimpeded to the outlet.

Most prior fill and spill observations at the soil-bedrock or soil-argillic interface have reported connectivity as discrete flow networks – almost channel like in their flow architecture (Tromp-van Meerveld and McDonnell, 2006; Hopp and McDonnell, 2009; Graham and McDonnell, 2010; Williams et al., 2013). By contrast, our fill and spill connectivity across this frozen hillslope occurred as a set of more amorphous locations of ponded water that intermittently and individually connected to the hillslope outlet (analogous to wetland connectivity on the Prairies; Leibowitz and Vining, 2003). These areas of ponded water exhibited heightened infiltration and soil water recharge beyond that exhibited by the general, gently-sloping hillslope area. This is akin to enhanced groundwater recharge observed under bedrock depressions at the soil-bedrock interface (Appels et al., 2015).

Finally, the four distinct stages in the evolution of meltwater inputs to the soil surface and runoff outputs from the hillslope can be explained by the pattern and rates of snowmelt (where the pattern exhibits a high spatial variability and the rates exhibit a high temporal variability) onto the frozen, reduced-infiltrability soil, and the pattern and layout of the micro-, meso-, and macro-topographic features:

- During Stage 1 (9th–12th March), snowmelt started to accumulate in the furrows, with no resulting hillslope runoff.
- In Stage 2 (13th–15th March), snowmelt continued to accumulate in the furrows and to be routed through each of the five flowpath systems. In flowpath systems 1 and 2, snowmelt water could then flow uninterrupted to the outlet, which generated the first hillslope runoff and low hillslope runoff ratios. Meanwhile, ponded water was accumulating behind the downslope barriers at the mouths of flowpath systems 3, 4, and 5.
- In Stage 3 (16th March), high volumes of snowmelt caused the water ponding at the mouths of flowpath systems 3, 4, and 5 to reach surface storage capacity and spill over their downslope barriers. This connected the upper region of the hillslope with the lower region, creating continuous flowpaths that connected all five flowpath systems to the hillslope outlet with a resultant instantaneous increase in runoff and high runoff ratios. Melt rates were highest in the upper region of the hillslope, which ensured the downslope depressions were continually fed, the surface storage capacity exceeded, and hillslope-wide connectivity maintained for 3–4 h. Following this, the ponded water fell below the downslope barriers and disconnected the upper two-thirds of the hillslope from the outlet.
- During Stage 4 (17th March onwards), low runoff resulted from slower, prolonged snowmelt, routed via micro-topography to the hillslope outlet from the remaining snow cover in the sheltered coulees over the lower third of the hillslope. The ground rapidly began to thaw from 17th March, enabling the remaining ponded water to readily infiltrate and contribute to soil water recharge. Overall, these four stages exhibited a dynamic contributing area – a feature of connectivity and fill and spill (Martin et al., 1983; Shaw et al., 2012). The contributing area was largely restricted to the lower third of the hillslope, but briefly extended to the entire hillslope on 16th March when widespread ponded water was connected to the hillslope outlet, before it contracted back again to the lower region of the hillslope.

5.3. Soil moisture based metrics of connectivity perform poorly for frozen hillslopes

Soil water content is critically important for soil infiltrability and hillslope runoff in general (*e.g.* Horton, 1933), over frozen ground on the Prairies (Granger et al., 1984; Zhao and Gray, 1999), and at this site in particular (Coles, 2017). Despite this, because the soil water content showed very little spatial variability, the spatial patterning of soil water content likely had little effect on the spatial variation in ponded water development and flowpath distribution. The hillslope's observed mean autumn surface soil water content was 0.15. If the soil was on average much drier at the time of freezing, we likely would have seen greater hillslope-wide infiltration, longer time for surface depressions to fill and then spill (if at all), and a delayed and damped increase in the delivery of water when connectivity was achieved. The opposite would have been true for a much wetter hillslope. There is some evidence of this at this site, where long-term runoff ratios were generally higher over wetter soils (likely a result of reduced infiltration) (Coles, 2017). However, this was mediated by the volume of surface depression storage such that runoff ratios were typically lower when there was a high surface depression storage even when the soils were wet (Coles, 2017).

Metrics that use the spatial arrangement of hillslope or catchment soil moisture as indicators of connectivity – because of the way stores of water fill up to generate hydrological connections (Tetzlaff et al., 2011; Bracken et al., 2013) – are likely not helpful for these frozen soils where there is little spatial variation over the hillslope. Further, for what little measured variability there was in soil water content, it was not related to topographic position. This could be attributed to the relatively low relief, and the influence of evapotranspiration in reducing the variability across the hillslope. At a similar prairie site, Peterson (2016) also observed that soil water content was not correlated with topographic relief. They also noted that soil water content variability was much higher under wetter conditions, yet still not related to topographic position (Peterson, 2016). Soil water content might have an effect on ponded water and flowpath formation if a more undulating site froze soon after rainfall (where side slopes might freeze dry and swales might freeze wet). We have not observed such effects, however. Analyses that use terrain to infer soil moisture and by extension flowpaths and connectivity (*e.g.* Beven and Kirkby, 1979; Lane et al., 2009) might reasonably accurately determine frozen ground flowpaths, but likely only due to structural routing of the water, rather than any topographically-induced differences in soil moisture. For example, our testing of the topographic wetness index (TWI; Beven and Kirkby, 1979; Fig. 8) unsurprisingly produced mapped results very similar to FA (Fig. 2b). The TWI metric does not incorporate any metric for downslope impedance, which the

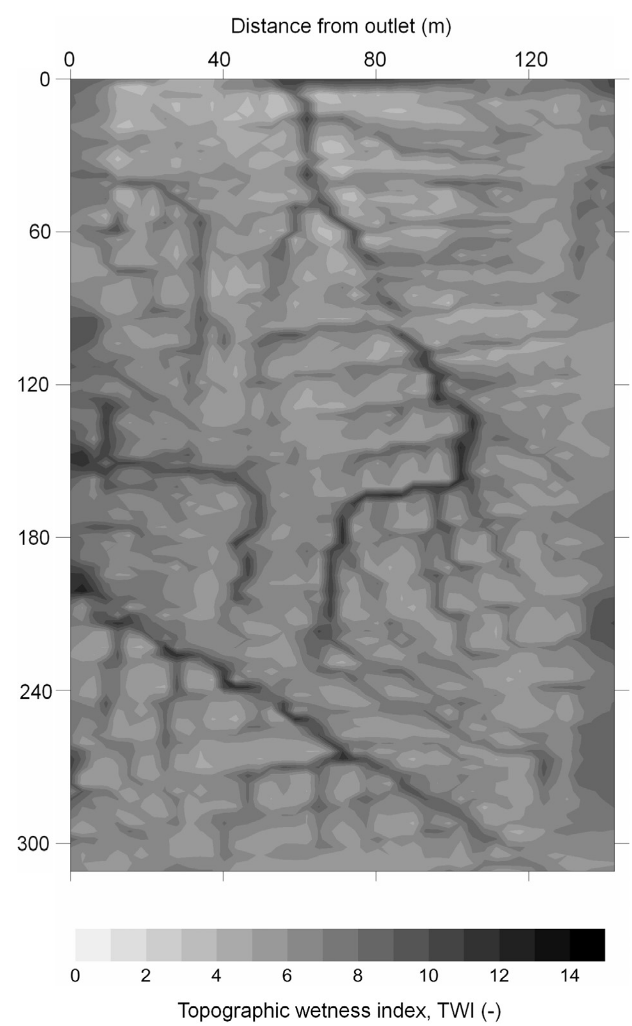

Fig. 8. Spatial map of the topographic wetness index (TWI).

use of DI here has shown to be an important component in the routing of flow and connectivity via fill and spill.

Previous work at this site has shown that a lumped approach can indeed be fruitful for predicting the seasonal runoff response (*e.g.* the decision tree model of Coles, 2017). We have shown here, though, that in order to understand and predict sub-seasonal time-scale (daily, hourly or weekly) runoff responses then distributed topographic data, distributed snowmelt data, frozen soil infiltration capacity data, and hillslope-average soil water content data are needed. Having determined that the fill and spill mechanism dictates hillslope runoff response for snowmelt over frozen ground, and given the underlying phenomenological similarities in fill and spill runoff generation processes at different partitioning surfaces (McDonnell, 2013; Ameli et al., 2015), then we can also look to existing fill and spill modeling approaches, just as Ameli et al. (2015) used an overland flow model to predict hillslope-scale subsurface flow. Existing fill and spill-like approaches could greatly improve predictions of wetland recharge, flooding, and water availability, for the dominant runoff-producing event of the year on the northern Great Plains. Appels et al. (2011) and Chu et al. (2013) developed numerical models to explore the effects of spatial organization of meso- and micro-topographic features on flowpath convergence, connectivity, and runoff. Interestingly, these plot- and hillslope-scale ponding and redistribution models are numerically very similar (save for their treatments of infiltration) to a physically-based landscape-scale model devised by Shook et al. (2013) to simulate surface storage dynamics in prairie wetlands that have been shown to connect and disconnect via the fill and spill mechanism (Leibowitz and Vining, 2003; Shaw et al., 2012; Leibowitz et al., 2016). Such approaches might therefore be adopted for the modeling of hillslope runoff response for snowmelt over frozen ground.

6. Conclusion

We examined snowmelt-runoff processes for the 2014 snowmelt season at a 46,600 m^2 hillslope site on the northern Great Plains. The fill and spill mechanism appears to explain the generation of snowmelt-runoff over frozen ground. Our main evidence for fill and spill is: 1) the contrast between the uniformly-frozen soil's low infiltration capacity and the relatively fast rates of snowmelt delivery to the soil surface that generated water beneath the snow at the soil surface and then accumulated in surface depressions; 2) stable isotope analysis of water showed that runoff water was event snowmelt water with limited mixing with pre-event soil water; and 3) observations of ponded water and flowpaths that matched our predictions of fill and spill activity from digital topographic analyses that combined flow accumulation and downslope indices. We observed nested filling at the micro- and *meso*-scale, followed by macro-scale spilling, where large patches of ponded water coalesced to drive an instantaneous increase in hillslope runoff. The identification of fill and spill as a mechanism to explain meltwater runoff from shallow, frozen hillslopes supports similar findings from peat-dominated permafrost sites in northern Canada where the frost table acts as an impeding layer, and has widespread implications for other areas of the northern Great Plains and similar low-angled, snowmelt-dominated, frozen regions.

Acknowledgements

We are grateful to Brian McConkey for useful ongoing discussions. Kelsey Brandt and Evan Powell (Swift Current Research and Development Centre, Agriculture and Agri-Food Canada), and Bruce Johnson, Willemijn Appels, Rosa Brannen, Kim Janzen, Chris Gabrielli, and Jaivime Evaristo (Global Institute for Water Security) provided valuable help in the field. The digital elevation data available for the site are a result of the surveying efforts of Mark Russell, Warren Helgason, and Amber Peterson. We thank two anonymous reviewers and the *Journal of Hydrology* editorial team for their useful comments. This research was funded by the Global Institute for Water Security, as well as an NSERC Discovery Grant and Accelerator Grants to JJM.

References

Ali, G.A., Roy, A.G., 2009. Revisiting hydrologic sampling strategies for an accurate assessment of hydrologic connectivity in humid temperate systems. Geography Compass 3, 350–374.
Ameli, A.A., Craig, J.R., McDonnell, J.J., 2015. Are all runoff processes the same? Numerical experiments comparing a Darcy-Richards solver to an overland flow-based approach for subsurface storm runoff simulation. Water Resour. Res. 51. https://doi.org/10.1002/2015WR017199.
Appels, W.M., Bogaart, P.W., van der Zee, S.E.A.T.M., 2011. Influence of spatial variations of microtopography and infiltration on surface runoff and field scale hydrological connectivity. Adv. Water Resour. 34, 303–313.
Appels, W.M., Graham, C.B., Freer, J.E., McDonnell, J.J., 2015. Factors affecting the spatial pattern of bedrock groundwater recharge at the hillslope scale. Hydrol. Process. 29 (21), 4594–4610.
Betson, R., 1964. What is watershed runoff? J. Geophys. Res. 69 (8), 1541–1552.
Beven, K.J., Kirkby, M.J., 1979. A physically based, variable contributing area model of basin hydrology. Hydrol. Sci. Bull. 24 (1), 43–69.
Bracken, L.J., Croke, J., 2007. The concept of hydrological connectivity and its contribution to understanding runoff dominated geomorphic systems. Hydrol. Process. 21, 1749–1763.
Bracken, L.J., Wainwright, J., Ali, G.A., Tetzlaff, D., Smith, M.W., Reaney, S.M., Roy, A. G., 2013. Concepts of hydrological connectivity: Research approaches, pathways and future agendas. Earth Sci. Rev. 119, 17–34.
Brannen, R., Spence, C., Ireson, A., 2015. Influence of shallow groundwater-surface water interactions on hydrological connectivity and water budget of a wetland complex. Hydrol. Process. 29 (18), 3862–3877.
Burt, T.P., Williams, P.J., 1976. Hydraulic conductivity in frozen soils. Earth Surf. Proc. Land. 1 (4), 349–360.
Carey, S.K., Woo, M., 2001. Slope runoff processes and flow generation in a subarctic, subalpine catchment. J. Hydrol. 253 (1–4), 110–129.
Cessna, A.J., McConkey, B.G., Elliott, J.A., 2013. Herbicide transport in surface runoff from conventional and zero-tillage fields. J. Environ. Qual. 42 (3). 782 93.
Chu, X., Yang, J., Chi, Y., Zhang, J., 2013. Dynamic puddle delineation and modeling of puddle-to-puddle filling-spilling-merging-splitting overland flow processes. Water Resour. Res. 49, 3825–3829.
Coles, A.E., 2017. Runoff generation over seasonally-frozen ground: trends, patterns, and processes. Ph.D. Thesis, Saskatoon: University of Saskatchewan. (Available at: http://hdl.handle.net/10388/7790).
Darboux, F., Davy, P., Gascuel-Odoux, C., Huang, C., 2002. Evolution of soil surface roughness and flowpath connectivity in overland flow experiments. Catena 46 (2–3), 125–139.
Devito, K., Creed, I., Gan, T., Mendoza, C., Petrone, R., Silins, U., Smerdon, B., 2005. A framework for broad-scale classification of hydrologic response units on the Boreal Plain: is topography the last thing to consider? Hydrol. Process. 19 (8), 1705–1714.
Du, E., Jackson, C.R., Klaus, J., McDonnell, J.J., Griffiths, N.A., Williamson, M.F., Greco, J.L., Bitew, M., 2016. Interflow dynamics on a low relief forested hillslope: Lots of fill, little spill. J. Hydrol. 534, 648–658.
Eriksson, D., Whitson, M., Luce, C.H., Marshall, H.P., Bradford, J., Benner, S.G., Black, T., Hetrick, H., McNamara, J.P., 2013. An evaluation of the hydrologic relevance of lateral flow in snow at hillslope and catchment scales. Hydrol. Process. 27, 640–654.
Fang, X., Minke, A., Pomeroy, J., Brown, T., Westbrook, C., Guo, X., Guangul, S., 2007. A Review of Canadian Prairie Hydrology: Principles, Modelling and Response to Land Use and Drainage Change. Centre for Hydrology Report #2, Saskatoon: University of Saskatchewan.
Graham, C.B., McDonnell, J.J., 2010. Hillslope threshold response to rainfall: (2) Development and use of a macroscale model. J. Hydrol. 393, 77–93.
Granger, R., Gray, D., Dyck, G., 1984. Snowmelt infiltration to frozen prairie soils. Can. J. Earth Sci. 21 (6), 669–677.
Grayson, R., Blöschl, G., 2001. Spatial Patterns in Catchment Hydrology. Cambridge University Press, Cambridge.
Gupta, H.V., Sorooshian, S., 1997. The challenges we face: panel discussion on snow, p. 183–187 in Sorooshian, S., Gupta, H.V., and Rodda, J.C. (eds.). Land Surface Processes in Hydrology: Trials and Tribulations of Modeling and Measuring. NATO ASI Series, Vol. I 46. Verlag Berlin Heidelberg New York: Springer.
Hewlett, J.D., Hibbert, A.R., 1967. Factors affecting the response of small watersheds to precipitation in humid areas. In: Sopper, W.E., Lull, H.W. (Eds.), Forest Hydrology. Pergamon Press, New York, pp. 275–290.
Hjerdt, K.N., McDonnell, J.J., Seibert, J., Rodhe, A., 2004. A new topographic index to quantify downslope controls on local drainage. Water Resour. Res. 40, W05602. https://doi.org/10.1029/2004WR003130.

Hopp, L., McDonnell, J.J., 2009. Connectivity at the hillslope scale: Identifying interactions between storm size, bedrock permeability, slope angle and soil depth. J. Hydrol. 376, 378–391.
Horton, R.E., 1933. The role of infiltration in the hydrologic cycle. Trans. Am. Geophys. Union 14, 446–460.
Kane, D.L., Bredthauer, S.R., Stein, J., 1981. Subarctic snowmelt runoff generation, p. 591–601 in Vinson, T.S. (ed.) Proceedings of the Specialty Conference on the Northern Community. Seattle, Washington: American Society of Civil Engineers.
Jackson, C.R., Du, E., Klaus, J., Griffiths, N.A., Bitew, M., McDonnell, J.J., 2016. Interactions among hydraulic conductivity distributions, subsurface topography, and transport thresholds revealed by a multitracer hillslope irrigation experiment. Water Resour. Res. 52 (8), 6186–6206. https://doi.org/10.1002/2015WR018364.
James, A.L., Roulet, N.T., 2007. Investigating hydrologic connectivity and its association with threshold change in runoff response in a temperate forested watershed. Hydrol. Process. 21 (25), 3391–3408.
James, A.L., McDonnell, J.J., Tromp-van Meerveld, H.J., Peters, N.E., 2010. Gypsies in the palace: experimentalist's view on the use of 3-D physics-based simulation of hillslope hydrological response. Hydrol. Process. 24 (26), 3878–3893.
Jenson, S.K., Domingue, J.O., 1988. Extracting topographic structure from digital elevation data for geographic information system analysis. Photogramm. Eng. Remote Sens. 54 (11), 1593–1600.
Lane, S.N., Reaney, S.M., Heathwaite, A.L., 2009. Representation of landscape hydrological connectivity using a topographically driven surface flow index. Water Resour. Res. 45, W08423. https://doi.org/10.1029/2008WR007336.
Leibowitz, S., Vining, K., 2003. Temporal connectivity in a prairie pothole complex. Wetlands 23 (1), 13–25.
Leibowitz, S.G., Mushet, D.M., Newton, W.E., 2016. Intermittent surface water connectivity: fill and spill vs. fill and merge dynamics. Wetlands 36, 323–342.
Martin, F.R.J., Mowchenko, F.M., Meid, P.O., 1983. The determination of gross and effective drainage areas in the Prairie Provinces. Hydrology Report # 104, Prairie Farm Rehabilitation Administration: Agriculture and Agri-food Canada.
McDonnell, J.J., 2013. Are all runoff processes the same? Hydrol. Process. 27, 4103–4111.
Orlowski, N., Pratt, D.L., McDonnell, J.J., 2016. Intercomparison of soil pore water extraction methods for stable isotope analysis. Hydrol. Process. 30 (19), 3434–3449. https://doi.org/10.1002/hyp.10870.
Penna, D., Tromp-van Meerveld, H.J., Gobbi, A., Borga, M., Dalla Fontana, G., 2011. The influence of soil moisture on threshold runoff generation processes in an alpine headwater catchment. Hydrol. Earth Syst. Sci. 15, 689–702.
Peterson, A.M., 2016. Field-scale root-zone soil moisture: spatio-temporal variability and mean estimation. Unpublished MS Thesis, Saskatoon: University of Saskatchewan.
Pomeroy, J.W., Gray, D.M., Brown, T., Hedstrom, N.R., Quinton, W.L., Granger, R.J., Carey, S.K., 2007. The cold regions hydrological model: a platform for basing process representation and model structure on physical evidence. Hydrol. Process. 21, 2650–2667.
Quinton, W.L., Marsh, P., 1999. A conceptual framework for runoff generation in a permafrost environment. Hydrol. Process. 13 (16), 2563–2581.
Quinton, W.L., Carey, S.K., Goeller, N.T., 2004. Snowmelt runoff from northern alpine tundra hillslopes: major processes and methods of simulation. Hydrol. Earth Syst. Sci. 8 (5), 877–890.
Reaney, S.M., Bracken, L.J., Kirkby, M.J., 2014. The importance of surface controls on overland flow connectivity in semi-arid environments: results from a numerical experimental approach. Hydrol. Process. 28 (4), 2116–2128.
Sarma, D.D., 2009. Geostatistics with Applications in Earth Sciences. Springer, The Netherlands.
Sayama, T., McDonnell, J.J., Dhakal, A., Sullivan, K., 2011. How much water can a watershed store? Hydrol. Process. 25, 3899–3908.
Seifert, W., 2014. Factors affecting the spatial pattern of infiltration capacity at the hillslope scale. Unpublished MSc thesis, Bayreuth: University of Bayreuth.
Shanley, J.B., Hjerdt, K.N., McDonnell, J.J., Kendall, C., 2003. Shallow water table fluctuations in relation to soil penetration resistance. Ground Water 41 (7), 964–972.
Shaw, D.A., Vanderkamp, G., Conly, F.M., Pietroniro, A., Martz, L., 2012. The fill-spill hydrology of prairie wetland complexes during drought and deluge. Hydrol. Process. 26, 3147–3156.
Shook, K.R., Pomeroy, J.W., 2011. Memory effects of depressional storage in Northern Prairie hydrology. Hydrol. Process. 25 (25), 3890–3898.
Shook, K., Pomeroy, J.W., Spence, C., Boychuk, L., 2013. Storage dynamics simulations in prairie wetland hydrology models: evaluation and parameterization. Hydrol. Process. 27 (13), 1875–1889.
Sivapalan, M., 2005. Pattern, process and function: elements of a unified theory of hydrology at the catchment scale. In: Anderson, M.G. (Ed.), Encyclopaedia of hydrological sciences. Wiley, Chichester, pp. 193–219.
Spence, C., 2010. A paradigm shift in hydrology: storage thresholds across scales influence catchment-runoff generation. Geography Compass 47 (7), 819–833.
Spence, C., Woo, M.-K., 2003. Hydrology of subarctic Canadian shield: soil-filled valleys. J. Hydrol. 279, 151–156.
Stichling, W., Blackwell, S.R., 1957. Drainage area as a hydrologic factor on the Glaciated Canadian prairies. Ontario: IUGG Proceedings.
Suzuki, K., Kubota, J., Ohata, T., Vuglinsky, V., 2005. Influence of snow ablation and frozen ground on spring runoff generation in the Mogot Experimental Watershed, southern mountainous taiga of eastern Siberia. Nord. Hydrol. 37 (1), 21–29.
Tetzlaff, D., McNamara, J.P., Carey, S.K., 2011. Measurements and modelling of storage dynamics across scales. Hydrol. Process. 25, 3831–3835.
Troch, P.A., Carrillo, G.A., Heidbuchel, I., Rajagopal, S., Switanek, M., Volkmann, T.H. M., Yaeger, M., 2008. Dealing with landscape heterogeneity in watershed hydrology: A review of recent progress toward new hydrological theory. Geography Compass 2, 1–18.
Tromp-van Meerveld, H.J., McDonnell, J.J., 2006. Threshold relations in subsurface stormflow: 2. The fill and spill hypothesis. Water Resour. Res. 42 (2), 1–11.
Western, A.W., Blöschl, G., Grayson, R.B., 2001. Toward capturing hydrologically significant connectivity in spatial patterns. Water Resour. Res. 37 (1), 83–97.
Williams, T.J., Quinton, W.L., Baltzer, J.L., 2013. Linear disturbances on discontinuous permafrost: implications for thaw-induced changes to land cover and drainage patterns. Environ. Res. Lett. 8. https://doi.org/10.1088/1748-9326/8/2/025006.
Williamson, M.J., 2016. A critical evaluation of the Hydra Probe for use in the validation of remote sensing soil freeze/thaw products. Unpublished MS Thesis, Guelph: University of Guelph.
Wright, N., Hayashi, M., Quinton, W.L., 2009. Spatial and temporal variations in active layer thawing and their implication on runoff generation in peat-covered permafrost terrain. Water Resour. Res. 45, W05414. https://doi.org/10.1029/2008WR006880.
Zhao, L., Gray, D.M., 1999. Estimating snowmelt infiltration into frozen soils. Hydrol. Process. 13, 1827–1842.
Zheng, X., Van Liew, M.W., Flerchinger, G.N., 2001. Experimental study of the infiltration into a bean stubble field during seasonal freeze-thaw period. Soil Sci. 166 (1), 3–10.